# Conductivity and redox stability of double perovskite oxide SrCaFe1+ xMo1– xO6–δ (x= 0.2, 0.4, 0.6)

**Cowin, PI, Lan, R, Petit, CTG & Tao, S**



**Original citation:**
Cowin, PI, Lan, R, Petit, CTG & Tao, S 2015, 'Conductivity and redox stability of double perovskite oxide SrCaFe1+ xMo1–xO6–δ (x= 0.2, 0.4, 0.6)' *Materials Chemistry and Physics*, vol 168, pp. 50-57
https://dx.doi.org/10.1016/j.matchemphys.2015.10.056

DOI 10.1016/j.matchemphys.2015.10.056
ISSN 0254-0584

Publisher: Elsevier

Materials Chemistry and Physics 168 (2015) 50–57

Contents lists available at ScienceDirect

Materials Chemistry and Physics

journal homepage: www.elsevier.com/locate/matchemphys

# Conductivity and redox stability of double perovskite oxide $SrCaFe_{1+x}Mo_{1-x}O_{6-\delta}$ (x = 0.2, 0.4, 0.6)

Peter I. Cowin [b], Rong Lan [a], Christophe T.G. Petit [b], Shanwen Tao [a, b, *]

[a] School of Engineering, University of Warwick, Coventry CV4 7AL, UK
[b] Department of Chemical & Process Engineering, University of Strathclyde, Glasgow G1 1XJ, UK

## HIGHLIGHTS

- New perovskite oxides $SrCaFe_{1+x}Mo_{1-x}O_{6-\delta}$ (x = 0.2, 0.4, 0.6) synthesised.
- The conductivity of $SrCaFe_{1.2}Mo_{0.8}O_{6-\delta}$ in 5% $H_2$/Ar was around 73.5 $Scm^{-1}$.
- The conductivity of these compounds relies on high temperature reduction.

## ARTICLE INFO

*Article history:*
Received 10 March 2015
Received in revised form
30 September 2015
Accepted 24 October 2015
Available online 14 November 2015

*Keywords:*
Ceramics
Inorganic compounds
Oxides
Electrical conductivity

## ABSTRACT

A series of new double perovskite oxides $SrCaFe_{1+x}Mo_{1-x}O_{6-\delta}$ (x = 0.2, 0.4, 0.6) were synthesised by solid state reaction method. Synthesis of $SrCaFe_{1+x}Mo_{1-x}O_{6-\delta}$ (x = 0.2, 0.4, 0.6) were achieved above 700 °C in 5% $H_2$/Ar, albeit with the formation of impurity phases. Introduction of calcium to $Sr_2Fe_{1+x}Mo_{1-x}O_{6-\delta}$ (x = 0.2, 0.4, 0.6) was not successful in simultaneously improving the conductivity of these compounds, with a significant reduction in the formability observed with increasing calcium content. Phase stability upon redox cycling was not observed for $SrCaFe_{1+x}Mo_{1-x}O_{6-\delta}$ (x = 0.2, 0.4, 0.6). Redox cycling of $SrCaFe_{1+x}Mo_{1-x}O_{6-\delta}$ (x = 0.2, 0.4, 0.6) demonstrates a strong dependence on high temperature reduction to achieve high conductivities, with re-reduction at lower temperatures attaining between 0.1% and 58.4% of the initial conductivity observed after high temperature reduction. The conductivity of $SrCaFe_{1.2}Mo_{0.8}O_{6-\delta}$ in 5%$H_2$/Ar between 300 °C and 500 °C was around 73.5 $Scm^{-1}$. The reliance of these compounds on high temperature reduction is expected to limit their utility as SOFC anode materials, as the vulnerability to oxidation can have disastrous consequence for fuel cell durability.



## 1. Introduction

Development of $Sr_2(TM)MoO_{6-\delta}$ (TM = Mn, Mg, Fe, Co, Ni, Cu, Zn) as potential anode materials has been the subject of a substantial body of research [1–5]. Whilst reasonable fuel cell performance has been achieved using $Sr_2MgMoO_{6-\delta}$ (642 $mWcm^{-2}$ at 750 °C in pure $H_2$) [1], $Sr_2MnMoO_{6-\delta}$ (467 $mWcm^{-2}$ at 750 °C in pure $H_2$) [1], $Sr_2CoMoO_{6-\delta}$ (1017 $mWcm^{-2}$ at 800 °C in pure $H_2$) [6] and $Sr_2FeMoO_{6-\delta}$ (412 $mWcm^{-2}$ at 750 °C in pure $H_2$) [7]anodes, of these compounds only $Sr_2MgMoO_{6-\delta}$ (SMMO) has been proven to be redox stable [8]. Despite achieving redox stability, the chemical reactivity of SMMO with common electrolytes, such as LSGM and YSZ, limits its utility [9,10].

Substitution of magnesium with iron has previously been shown to improve the conductivity, albeit with a reduction in the redox stability [8]. Xiao et al. improved both the formability and stability of $Sr_2FeMoO_{6-\delta}$ through an increase in the iron content of the sample, with $Sr_2Fe_{1.33}Mo_{0.66}O_{6-\delta}$ formed in at 800 °C in $H_2$, 300 °C below the synthesis temperature of $Sr_2FeMoO_{6-\delta}$ in 5% $H_2$/Ar [7,11]. The conductivity of $Sr_2Fe_{1.33}Mo_{0.66}O_{6-\delta}$ in 5% $H_2$/Ar ranges between 15 S $cm^{-1}$ and 30 S $cm^{-1}$ from 700 °C to 300 °C, sufficient for an IT-SOFC anode material, although the fuel cell performance only reached 268 $mWcm^{-2}$ at 700 °C in pure $H_2$. Further development of this series by Liu et al. formed $Sr_2Fe_{1.5}Mo_{0.5}O_{6-\delta}$ in air at 1000 °C and demonstrated high conductivity in both oxidising and reducing atmospheres [2]. Good performance of $Sr_2Fe_{1.5}Mo_{0.5}O_{6-\delta}$ as a symmetrical electrode was achieved, attaining ~500 $mWcm^{-2}$ at 800 °C in humidified $H_2$ with good stability over successive redox cycles.

* Corresponding author. School of Engineering, University of Warwick, UK.
*E-mail address:* S.Tao.1@warwick.ac.uk (S. Tao).

http://dx.doi.org/10.1016/j.matchemphys.2015.10.056

A-site substitution of alkaline earth metals was determined to cause a significant alteration of material properties, with a reduction in cation size (from Ba to Sr to Ca) causing an increase in the conductivity and a reduction in the material stability [7]. The increase in conductivity achieved through calcium substitution would be expected to improve anodic performance, although a significant improvement in the stability of the compound is required for use in IT-SOFCs [10,12]. To this end, in this study, a series of compounds of iron rich calcium iron molybdates, $Ca_2Fe_{1+x}Mo_{1-x}O_{6-\delta}$ (x = 0.2, 0.4, 0.6) and strontium calcium iron molybdate, $SrCaFe_{1+x}Mo_{1-x}O_{6-\delta}$ (x = 0.2, 0.4, 0.6), were synthesised to determine whether a simultaneous improvement of the conductivity and stability of these compounds was attainable.

## 2. Experimental information

### 2.1. Materials synthesis

$Ca_2Fe_{1+x}Mo_{1-x}O_{6-\delta}$ (x = 0.2, 0.4, 0.6) were prepared by solid state synthesis technique. Stoichiometric amounts of $CaCO_3$ (99% min, Alfa Aesar), $Fe_2O_3$ (99.5%, Alfa Aesar) and $MoO_3$ (99.5%, Alfa Aesar) were weighed and mixed in a planetary ball mill for 2 h prior to firing in air at 900 °C for 10 h. A second firing at 1200 °C in air for 50 h was then performed. For comparison, the samples fired at 1200 °C in air were further fired in 5% $H_2$/Ar at 700 °C for 10 h.

$SrCaFe_{1+x}Mo_{1-x}O_{6-\delta}$ (x = 0.2, 0.4, 0.6) were prepared by solid state synthesis technique. Stoichiometric amounts of $CaCO_3$ (99% min, Alfa Aesar),$SrCO_3$ (>99.9%, Sigma Aldrich), $Fe_2O_3$ (99.5%, Alfa Aesar) and $MoO_3$ (99.5%, Alfa Aesar) were weighed and mixed in a planetary ball mill for 2 h prior to firing in air at 900 °C for 10 h. Pellets of all the samples (ø ≈ 13 mm × 2 mm) were uniaxially pressed at 221 MPa and sintered in air at 1300 °C for 5 h. The as-prepared $SrCaFe_{1+x}Mo_{1-x}O_{6-\delta}$ samples were further fired in 5% $H_2$/Ar for 10 h at 700 °C and 1200 °C respectively.

### 2.2. Materials characterisation

Phase purity and crystal parameters of the samples were examined by X-ray diffraction (XRD) analysis using a PANalytical X'Pert PRO MPD Multipurpose diffractometer (Cu $K_{\alpha 1}$ radiation, λ = 1.5405 Å). GSAS [13] software was used to perform a least squares refinement of the lattice parameters of all suitable samples.

The densities of the pellets were determined from the measured mass and volume. Theoretical densities were calculated using experimental lattice parameters and the chemical formula of the sample. The relative densities were calculated from the actual and theoretical density values. The density of the pellets was 65–80% for $Ca_2Fe_{1+x}Mo_{1-x}O_{6-\delta}$ (x = 0.2, 0.4, 0.6) and 80% for $SrCaFe_{1+x}Mo_{1-x}O_{6-\delta}$ (x = 0.2, 0.4, 0.6).

Thermal analysis was conducted using a Stanton Redcroft STA 1500 Thermal Analyser on heating from room temperature to 800 °C and on cooling from 800 °C to room temperature in air, with a heating/cooling rate of 10 °C/min, and in 5% $H_2$/Ar, again with a heating/cooling rate of 10 °C/min, and with a flow rate of 50 mLmin$^{-1}$ for 5% $H_2$/Ar.

### 2.3. Conductivity measurements

Pellets for $SrCaFe_{1+x}Mo_{1-x}O_{6-\delta}$ (x = 0.2, 0.4, 0.6) were coated on opposing sides using silver paste after firing at 1200 °C for 8 h in 5% $H_2$/Ar. The conductivity of the samples was measured primarily in 5% $H_2$/Ar between 300 and 700 °C. Although pure $H_2$ is used in a hydrogen fuel cells, it is normally wet $H_2$ with 3%$H_2O$. The oxygen partial pressure of wet $H_2$ is at the same level as the un-humidified 5%$H_2$/Ar used in our conductivity measurement. Therefore the conductivity measured in 5%$H_2$/Ar in this study can provide a good reference for the conductivity in wet $H_2$ which is close to the fuel cell operating condition [14]. Secondary measurements over the same temperature range were conducted in air following an equilibration step of 12 h at 700 °C in air. Final measurements over the same temperature range were conducted after an equilibration step of 12 h at 700 °C in 5% $H_2$/Ar. Measurements were conducted using either an A.C. method utilising a Solartron 1455A frequency response analyser coupled to a Solartron 1470E potentiostat/galvanostat controlled by CellTest software over the frequency range 1 MHz–100 mHz or a DC method using a Solartron 1470E potentiostat/galvanostat controlled by CellTest software with an applied current of 1–0.1 A as described elsewhere [15–17].

## 3. Results and discussion

### 3.1. Synthesis of $Ca_2Fe_{1+x}Mo_{1-x}O_{6-\delta}$ and $SrCaFe_{1+x}Mo_{1-x}O_{6-\delta}$ (x = 0.2, 0.4, 0.6) in air and 5%$H_2$/Ar

Synthesis of single phase $Ca_2Fe_{1+x}Mo_{1-x}O_{6-\delta}$ (x = 0.2, 0.4, 0.6) compounds in air at 1200 °C was unsuccessful, with the formation of both $CaMoO_4$ (PDF: 01-077-2238, 29–351) and $Ca_2Fe_2O_5$ (PDF:

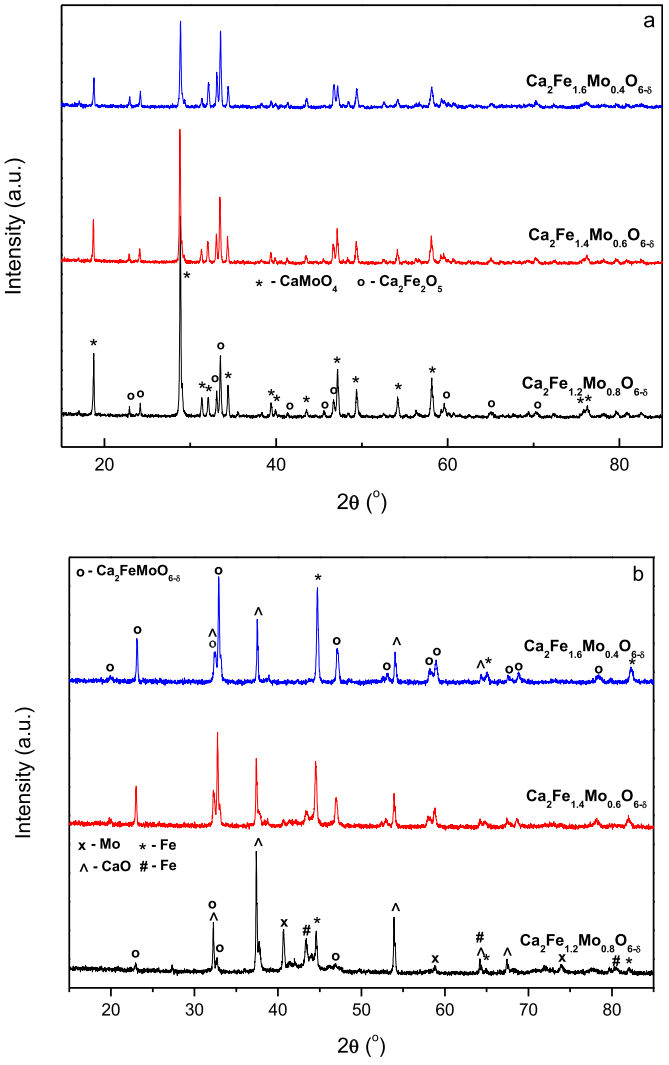


**Fig. 1.** XRD patterns of $Ca_2Fe_{1+x}Mo_{1-x}O_{6-\delta}$ (x = 0.2, 0.4 and 0.6) synthesised in air at 1200 °C (a) and 5%$H_2$/Ar at 1000 °C (b).

01-071-2108, 38–408) phases observed, Fig. 1(a). Previous research by Zhang et al. [7] indicated that formation of the calcium based compounds would require firing in reducing atmospheres, therefore it is somewhat unsurprising that synthesis of pure calcium materials in air was unsuccessful. The samples fired at 1200 °C in air were further fired in 5%$H_2$/Ar at 700 °C for 10 h. Formation of a single phase perovskite after firing at 700 °C in 5% $H_2$/Ar was also unsuccessful, with the presence of calcium oxide and pure iron phases observed for all compounds, Fig. 1(b). Comparison to the unreduced samples, Fig. 1(a), demonstrates that reduction causes degradation of the phases formed in air, likely due to reduction of the iron and molybdenum in the samples. This corresponds to previous reports which suggest that extended reduction of calcium iron molybdates at high temperatures will cause the exsolution of iron and molybdenum from the structure [18]. The differing phase fractions observed for this series could be related to the stability of the $Ca_2Fe_{1+x}Mo_{1-x}O_{6-\delta}$ phase, with increasing proportions of the desired phase evident with increasing iron content.

Synthesis of $SrCaFe_{1+x}Mo_{1-x}O_{6-\delta}$ (x = 0.2, 0.4, 0.6) in air was found to form a two phase mixture, with a primary double perovskite phase (Space Group (SG): *Fm-3m*) and a secondary $SrMoO_{4-\delta}$–based phase (PDF: 01-085-0809, SG: *I4/mmm*) observed for all compounds, Fig. 2. The formation of materials with the *Fm-3m* space group correlates with the observed structure of the iron rich strontium analogues previously synthesised by Liu et al. [19]. Due to the formation of the desired phase, comparison of these compounds to $Ca_2Fe_{1+x}Mo_{1-x}O_{6-\delta}$ (x = 0.2, 0.4, 0.6) demonstrates a significant improvement in the formability in air with increased strontium content.

### 3.2. Synthesis of $SrCaFe_{1+x}Mo_{1-x}O_{6-\delta}$ (x = 0.2, 0.4, 0.6) in 5%$H_2$/Ar at 700 °C and 1200 °C respectively

Simultaneous thermal analysis in 5% $H_2$/Ar of the samples formed in air, Fig. 3(a), exhibited a weight loss proportional to the iron content of the samples. This suggests that the primary element reduced during exposure to 5% $H_2$/Ar at this temperature is iron, from $Fe^{4+}$ to $Fe^{3+}$, and that reduction at higher temperatures, > 800 °C, is required for significant reduction of the molybdenum and subsequent formation of single phase perovskites. A small deviation in the DSC, Fig. 3(b), was observed for all compounds between

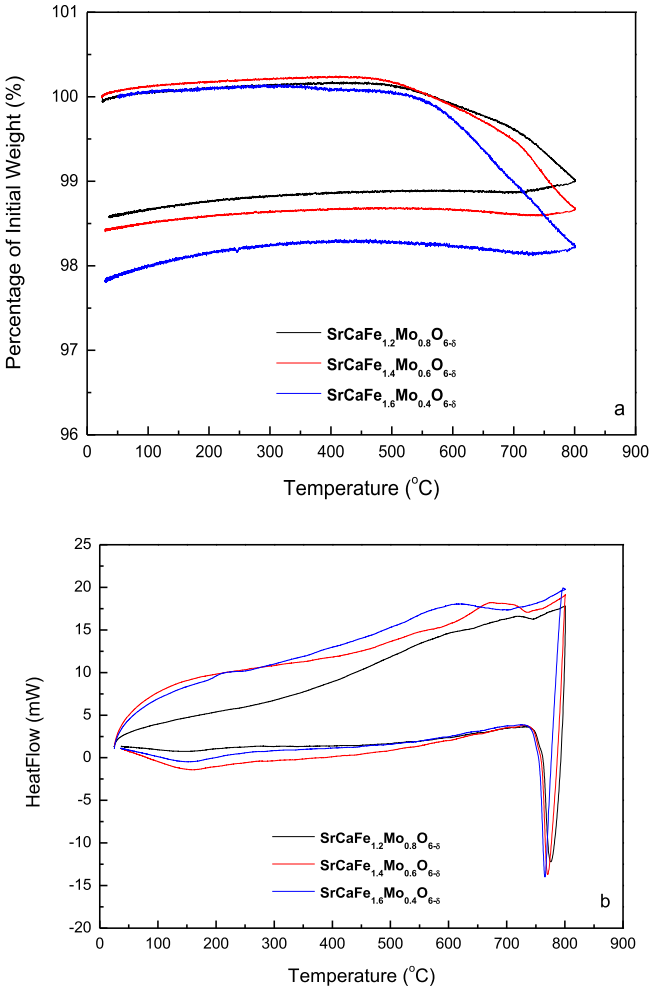


**Fig. 3.** Thermogravimetric analysis (a) and differential scanning calorimetry (b) of $SrCaFe_{1+x}Mo_{1-x}O_{6-\delta}$ (x = 0.2, 0.4 and 0.6) in 5% $H_2$/Ar.

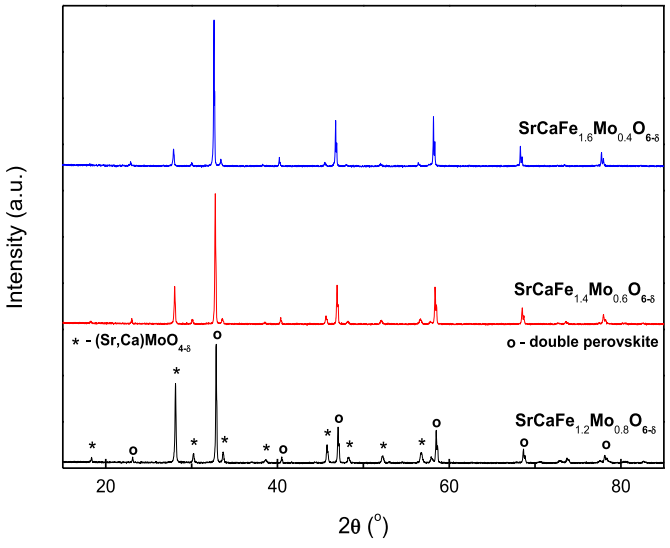


**Fig. 2.** XRD patterns of $SrCaFe_{1+x}Mo_{1-x}O_{6-\delta}$ (x = 0.2, 0.4 and 0.6) synthesised in air at 1300 °C.

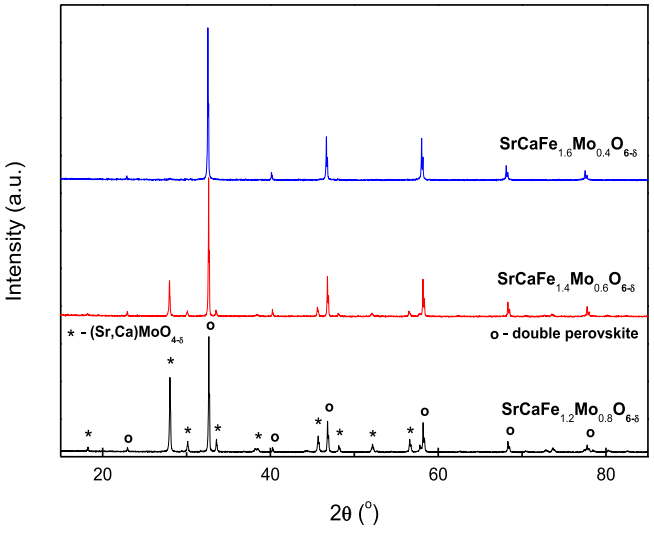


**Fig. 4.** XRD patterns of $SrCaFe_{1+x}Mo_{1-x}O_{6-\delta}$ (x = 0.2, 0.4 and 0.6) after reduction in 5% $H_2$/Ar at 700 °C.

550 °C and 750 °C, correlating with the induction of weight loss observed on the TGA.

Reduction of the samples at 700 °C in 5% $H_2$/Ar formed a single phase double perovskite for the iron rich $SrCaFe_{1.6}Mo_{0.4}O_{6-\delta}$ sample (PDF: *Fm-3m*), Fig. 4, although both $SrCaFe_{1.2}Mo_{0.8}O_{6-\delta}$ and $SrCaFe_{1.4}Mo_{0.6}O_{6-\delta}$ continued to exhibit the secondary $SrMoO_{4-\delta}$–based phase (PDF: 01-085-0809), with little change in the phase fraction. The formation of a single phase double perovskite for $SrCaFe_{1.6}Mo_{0.4}O_{6-\delta}$ at 700 °C in 5% $H_2$/Ar demonstrates an improvement in the formability over the pure calcium analogue.

Formation of mainly single phase double perovskites (SG: *Fm-3m*) was achieved for all compounds after reduction in 5% $H_2$/Ar at 1200 °C for 10 h, Fig. 5. The formation of the double perovskite phase at 1200 °C in 5% $H_2$/Ar was predicted to occur, as previous reports suggested that the formation of the less stable $Ca_2FeMoO_{6-\delta}$ phase was achieved at 1100 °C in 5% $H_2$/Ar [7]. As with reduction of the pure calcium analogue in 5% $H_2$/Ar at 700 °C for 10 h, exsolution of elemental iron (PDF: 6–696) was observed for all compounds, reducing with increasing iron content in the primary phase. A proportion of $Ca_2Fe_2O_5$ (PDF: 01-071-2108, 38–408) was also observed for sample $SrCaFe_{1.6}Mo_{0.4}O_{6-\delta}$. The proportion of the secondary phase in the synthesised materials was calculated as 2–8 wt% for iron and 24 wt% for $Ca_2Fe_2O_5$ through GSAS refinement of the phase fractions. Due to the proportion of these phases, elemental iron in the samples is considered to have a minimal effect on the preceding measurements, however the sizeable presence of $Ca_2Fe_2O_5$ in $SrCaFe_{1.6}Mo_{0.4}O_{6-\delta}$ must be considered in the analysis of the material properties.

GSAS refinement of the structure of these compounds, Table 1, demonstrated a non-linear increase in lattice parameters with increasing iron content. Both $SrCaFe_{1.2}Mo_{0.8}O_{6-\delta}$ and $SrCaFe_{1.4}Mo_{0.6}O_{6-\delta}$ exhibit similar lattice parameters with $SrCaFe_{1.6}Mo_{0.4}O_{6-\delta}$ exhibiting significantly higher lattice parameters. The higher lattice parameter noted for $SrCaFe_{1.6}Mo_{0.4}O_{6-\delta}$ may be due to the large proportion of the secondary phase and the corresponding inaccuracy associated with three phase refinements. GSAS plots of $SrCaFe_{1+x}Mo_{1-x}O_{6-\delta}$, x = 0.2, 0.4 and 0.6 after reduction in 5% $H_2$/Ar at 1200 °C are shown in Fig. 6.

### 3.3. Conductivity and redox stability of $SrCaFe_{1+x}Mo_{1-x}O_{6-\delta}$ (x = 0.2, 0.4, 0.6)

DC conductivity measurements of each of the $SrCaFe_{1+x}Mo_{1-x}O_{6-\delta}$ (x = 0.2, 0.4, 0.6) compounds exhibited high electronic conductivity, > 30 $Scm^{-1}$, between 300 °C and 700 °C in 5% $H_2$/Ar immediately after reduction at 1200 °C in 5% $H_2$/Ar, Fig. 7(a–c). Initial semiconducting behaviour was observed for $SrCaFe_{1.6}Mo_{0.4}O_{6-\delta}$ between 300 °C and 450 °C, $SrCaFe_{1.4}Mo_{0.6}O_{6-\delta}$ between 300 °C and 350 °C and $SrCaFe_{1.2}Mo_{0.8}O_{6-\delta}$ between 300 °C and 500 °C, exhibiting maximum conductivities of 64.8 $Scm^{-1}$, 60.6 $Scm^{-1}$ and 73.5 $Scm^{-1}$ respectively, with metallic conductivity was observed for all compounds above 500 °C. The conductivity of these compounds is comparable to those observed for $Sr_2Fe_{1.5}Mo_{0.5}O_{6-\delta}$ [20] and $Sr_2Fe_{1.33}Mo_{0.66}O_{6-\delta}$.achieved by Xiao et al. [11].

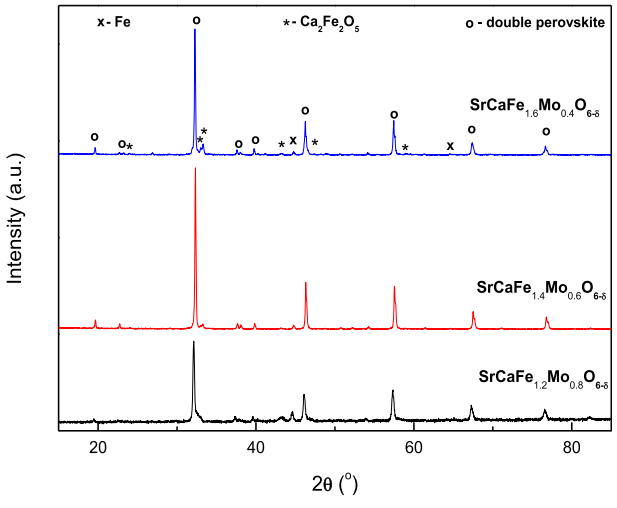


**Fig. 5.** XRD patterns of $SrCaFe_{1+x}Mo_{1-x}O_{6-\delta}$ (x = 0.2, 0.4 and 0.6) after reduction in 5% $H_2$/Ar at 1200 °C.

The metallic conductivity observed for all compounds above 500 °C is also found for $Ca_2FeMoO_{6-\delta}$ [18] and $Sr_2FeMoO_{6-\delta}$ [21] as a result of the delocalisation of electrons in the spin down band at the Fermi level. Band structure calculations of $Ca_{2-x}Sr_xFeMoO_{6-\delta}$ [22] exhibit a gap at the Fermi level between Fe 3d and Mo 4d states for the spin up structure, however the spin down structure exhibits a mixing of the Fe 3d, Mo 4d and O 2p bands at the Fermi level. Spin down electrons from either the Mo 4d or Fe 3d states are delocalised at the Fermi level, arising from $Mo^{5+}$ ($4\,d^1$) and $Fe^{3+}$ ($3\,d^5$), accounting for the observed metallic conductivity [7,18,21].

The high conductivity of $SrCaFe_{1.2}Mo_{0.8}O_{6-\delta}$, $SrCaFe_{1.4}Mo_{0.6}O_{6-\delta}$ and $SrCaFe_{1.6}Mo_{0.4}O_{6-\delta}$ after reduction in 5% $H_2$/Ar at 1200 °C suggests that delocalised electrons from $Mo^{5+}$ are unlikely to be the sole source of the metallic conductivity, as minimal variation in the electronic conductivity was observed despite significant variation in the molybdenum content.

The observed conductivity of $A_2FeMoO_{6-\delta}$ (A = Ca, Sr, Ba) [7] was linked to a potential double exchange mechanism, with conduction between $Fe^{3+}$-O-Mo-O-$Fe^{2+}$. Double-exchange mechanisms, as proposed by Zener [23], posit that electron transfer between ions in different oxidation states may be facilitated if the electron does not have to alter its spin state. Replacement of Mo with Fe in this mechanism would be expected to result in a reduction of the conductivity through reduction of the available percolation pathways, unless delocalisation of Fe electrons through $Fe^{2+}$-O-$Fe^{3+}$ exchange could also occur. Double exchange mechanisms have been observed previously for mixed valent iron in iron oxides [24], and, as iron is known to exist in a mixed valent state for $Ca_{2-x}Sr_xFeMoO_{6-\delta}$ [25], this provides a plausible explanation for the observed metallic conductivity. Band structure calculations and Mossbauer spectroscopy could be utilised to further elucidate the conduction mechanism for these compounds, however this is outside the scope of this enquiry.

Whilst metallic conductivity is observed for pure calcium molybdenum ferrites over the entire temperature range, a region of semiconductivity, as was observed for $SrCaFe_{1+x}Mo_{1-x}O_{6-\delta}$ (x = 0.2, 0.4, 0.6), has been observed previously for barium and strontium molybdenum ferrites [7]. Previous reports have attributed the initial region of semiconductivity observed for all compounds to either disorder of the iron and molybdenum or the presence of oxygen vacancies, causing Anderson localisation [21,26,27]. Anderson localisation is used to account for the absence of wave diffusion in a disordered medium and can account for electron localisation in materials when lattice disorder is sufficiently large. Under these conditions the mobility edge, the highest energy at which states are localised, occurs at a higher energy than the Fermi level, resulting in electron localisation. The transition to metallic conductivity could then be rationalised through a gradual increase of the Fermi level to a higher energy than the mobility edge, due to a reduction in the lattice disorder with increasing temperature [21].

Oxidation of these compounds at 700 °C significantly reduced the conductivity, to <0.1 $Scm^{-1}$, for all compounds, Fig. 7(a–c).

**Table 1**
Rietveld refinement and lattice parameters from GSAS refinement of $SrCaFe_{1+x}Mo_{1-x}O_{6-\delta}$ (x = 0.2, 0.4, 0.6) after reduction at 1200 °C in 5% $H_2$/Ar.

| | | $SrCaFe_{1.2}Mo_{0.8}O_{6-\delta}$ | $SrCaFe_{1.4}Mo_{0.6}O_{6-\delta}$ | $SrCaFe_{1.6}Mo_{0.4}O_{6-\delta}$ |
|---|---|---|---|---|
| $\chi^2$ | | 1.924 | 5.111 | 3.851 |
| Rp (%) | | 8.24 | 7.82 | 6.75 |
| wRp (%) | | 6.27 | 5.38 | 4.89 |
| Space Group | | *Fm-3m* | *Fm-3m* | *Fm-3m* |
| a (Å) | | 7.850(2) | 7.849(1) | 7.863(1) |
| V (Å$^3$) | | 483.8(5) | 483.6(2) | 486.1(2) |
| Fe (%) | | 7.8 | 2.4 | 1.7 |
| Space Group | | *Im-3m* | *Im-3m* | *Im-3m* |
| a (Å) | | 2.864(1) | 2.866(1) | 2.866(1) |
| $Ca_2Fe_2O_5$ (%) | | – | – | 24 |
| Space Group | | – | – | *Pcmn* |
| a (Å) | | – | – | 5.618(1) |
| b (Å) | | – | – | 14.905(3) |
| c (Å) | | – | – | 5.437(1) |
| Sr/Ca | x | 0.5 | 0.5 | 0.25 |
| | y | 0.5 | 0.5 | 0.25 |
| | z | 0.5 | 0.5 | 0.25 |
| | $U_{iso}$ | 0.007(2) | 0.005(1) | 0.002(1) |
| Fe | x | 0 | 0 | 0 |
| | y | 0 | 0 | 0 |
| | z | 0 | 0 | 0 |
| | $U_{iso}$ | 0.029(5) | 0.034(2) | 0.049(3) |
| Fe/Mo | x | 0.5 | 0.5 | 0.5 |
| | y | 0.5 | 0.5 | 0.5 |
| | z | 0.5 | 0.5 | 0.5 |
| | $U_{iso}$ | 0.038(3) | 0.003(1) | 0.002(1) |
| O | x | 0.243(2) | 0.257(1) | 0.266(1) |
| | y | 0 | 0 | 0 |
| | z | 0.5 | 0.5 | 0 |
| | $U_{iso}$ | 0.068(4) | 0.062(2) | 0.077(2) |

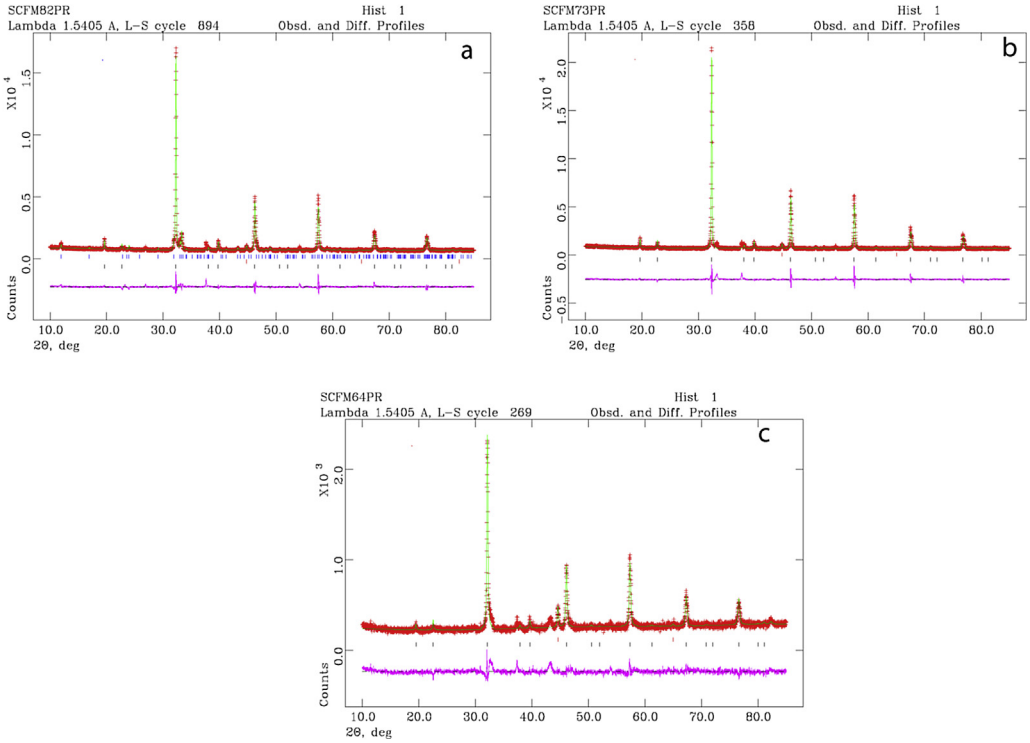


**Fig. 6.** GSAS plots of $SrCaFe_{1+x}Mo_{1-x}O_{6-\delta}$, x = 0.2 (a), x = 0.4 (b) and x = 0.6 (c) after reduction in 5% $H_2$/Ar at 1200 °C.

Compound oxidation of these materials favours the formation of $Fe^{3+}$ and $Mo^{6+}$, which reduces double exchange conduction through the reduction in mixed valence cations. The transition to semiconducting behaviour upon oxidation observed for these materials has been previously exhibited in $Sr_2FeMoO_{6-\delta}$ [21].

Reduction of the previously oxidised compounds at 700 °C in 5%

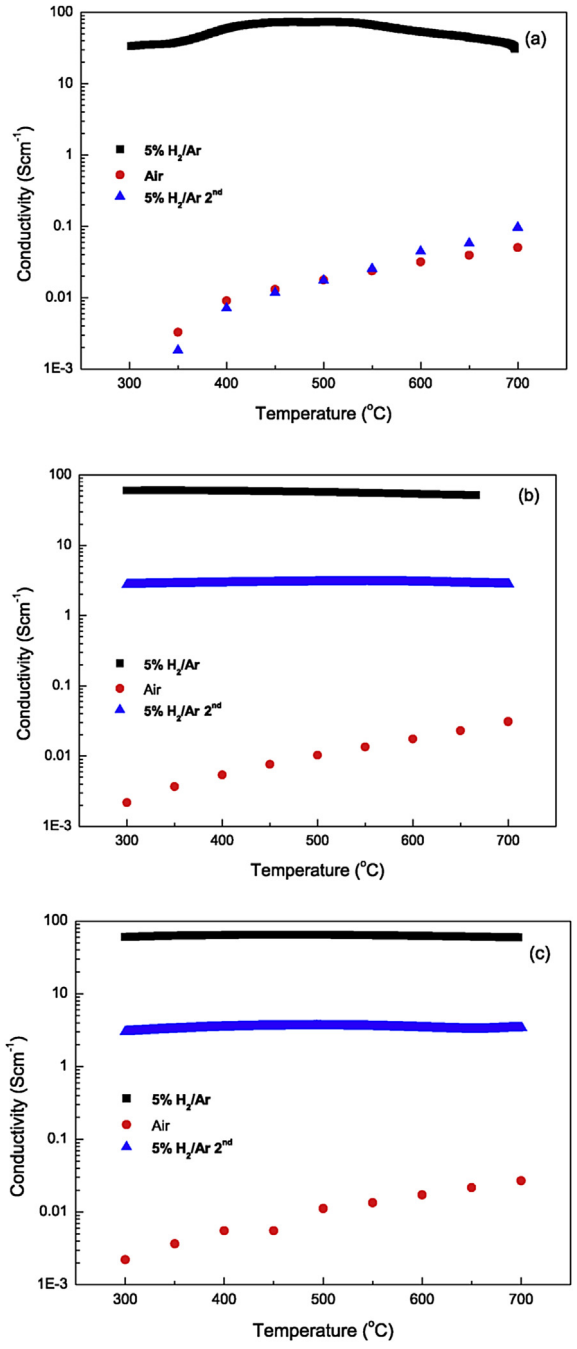


**Fig. 7.** Conductivity of $SrCaFe_{1+x}Mo_{1-x}O_{6-\delta}$, x = 0.2 (a), x = 0.4 (b) and x = 0.6 (c), in 5% $H_2$/Ar after reduction at 1200 °C in 5% $H_2$/Ar (black), in air after re-oxidation of the sample reduced at 1200 °C in 5% $H_2$/Ar (red) and in 5% $H_2$/Ar using the re-oxidised sample (blue).

$H_2$/Ar did not attain the high conductivity observed after reduction at 1200 °C, with both $SrCaFe_{1.6}Mo_{0.4}O_{6-\delta}$ and $SrCaFe_{1.4}Mo_{0.6}O_{6-\delta}$ retaining ~5% of the initial conductivity, whilst $SrCaFe_{1.2}Mo_{0.8}O_{6-\delta}$ only retained 0.3%. Although the conductivity exhibited after re-reduction at 700 °C is lower than previously observed, the initial semiconduction with a higher temperature transition to metallic conduction is still observed for both $SrCaFe_{1.6}Mo_{0.4}O_{6-\delta}$ and $SrCaFe_{1.4}Mo_{0.6}O_{6-\delta}$. This suggests that the same conduction mechanism occurs, however the magnitude of the conduction is reduced. As the ratio of both $Fe^{3+}/Fe^{2+}$ and $Mo^{6+}/Mo^{5+}$ is known to be highly dependent on the reducing atmosphere and temperature [18,21], it is expected that the reduction in the conductivity is a result of a lower degree of mixed valency due to the lower reduction temperature. The reduction of $Fe^{3+}$ to $Fe^{2+}$, the outer orbital changes from 3 $d^5$ to 3 $d^6$. The ions with high spin of 3 $d^5$ and low spin of 3 $d^6$ will not be conductive. The reduction of $Mo^{6+}$ (4 $d^0$) to $Mo^{5+}$ (4 $d^1$) will introduce an electron in the 4d orbital which can be an electron charge carrier thus makes the oxide conductive [3,4].

XRD of $SrCaFe_{1+x}Mo_{1-x}O_{6-\delta}$ (x = 0.2, 0.4, 0.6) after redox cycling, Fig. 8, exhibited differing impurity phases and phase fractions for all compounds. The $SrMoO_4$–based impurity phase (PDF: 01-085-0809) was noted for $SrCaFe_{1.4}Mo_{0.6}O_{6-\delta}$, CaO (PDF: 01-075-0264, 43–1001) was observed for $SrCaFe_{1.6}Mo_{0.4}O_{6-\delta}$, whilst $SrCaFe_{1.2}Mo_{0.8}O_{6-\delta}$ exhibited a $Ca_2Fe_2O_5$ (PDF: 01-071-2108, 38–408) impurity phase. GSAS analysis, Table 2, demonstrated a non-linear variation in lattice parameters likely due to the formation of the various secondary phases. GSAS plots of $SrCaFe_{1+x}Mo_{1-x}O_{6-\delta}$, x = 0.2, 0.4 and 0.6 after re-oxidation and re-reduction of the samples reduced in 5% $H_2$/Ar at 1200 °C as shown in Fig. 9. The lack of redox stability of these materials further reduces any possible utility of these materials for SOFC application.

## 4. Conclusion

Introduction of calcium to $Sr_2Fe_{1+x}Mo_{1-x}O_{6-\delta}$ (x = 0.2, 0.4, 0.6) was not successful in simultaneously improving the conductivity and stability of these compounds, with a significant reduction in the formability observed with increasing calcium content. Potassium substitution into $Sr_2Fe_{1+x}Mo_{1-x}O_{6-\delta}$ (x = 0.2, 0.4, 0.6) with the intention of increasing the formability and ionic conductivity was also unsuccessful, with no notable formability improvements observed.

Redox cycling of $SrCaFe_{1+x}Mo_{1-x}O_{6-\delta}$ (x = 0.2, 0.4, 0.6) demonstrates a strong dependence on high temperature reduction to achieve high conductivities, with re-reduction at lower temperatures attaining between 0.1% and 58.4% of the initial conductivity observed after high temperature reduction. The conductivity of $SrCaFe_{1.2}Mo_{0.8}O_{6-\delta}$ in 5%$H_2$/Ar between 300 °C and 500 °C was around 73.5 Scm$^{-1}$. The reliance of these compounds on high

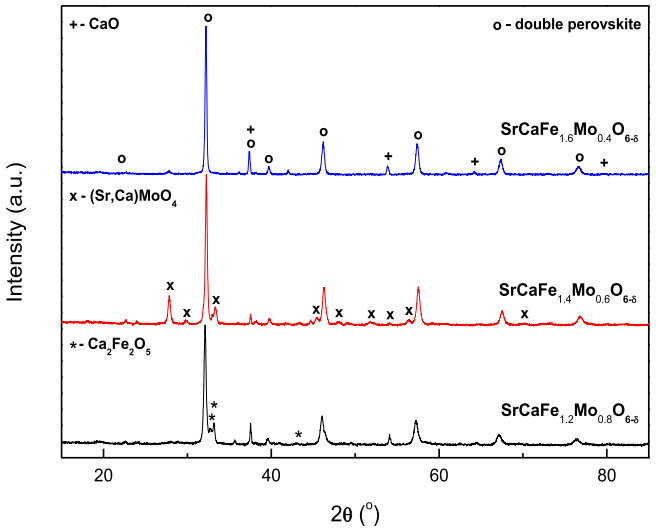


**Fig. 8.** XRD patterns of $SrCaFe_{1+x}Mo_{1-x}O_{6-\delta}$ (x = 0.2, 0.4 and 0.6) after re-oxidation and re-reduction of the samples reduced in 5% $H_2$/Ar at 1200 °C.

**Table 2**
Rietveld refinement and lattice parameters from GSAS refinement of $SrCaFe_{1+x}Mo_{1-x}O_{6-\delta}$ (x = 0.2, 0.4, 0.6) after re-oxidation and re-reduction at 700 °C in 5% $H_2$/Ar of the compounds previously reduced at 1200 °C in 5% $H_2$/Ar.

| | | $SrCaFe_{1.2}Mo_{0.8}O_{6-\delta}$ | $SrCaFe_{1.4}Mo_{0.6}O_{6-\delta}$ | $SrCaFe_{1.6}Mo_{0.4}O_{6-\delta}$ |
|---|---|---|---|---|
| $\chi^2$ | | 4.466 | 6.432 | 2.565 |
| Rp (%) | | 6.84 | 8.41 | 6.17 |
| wRp (%) | | 4.46 | 5.83 | 4.70 |
| Space Group | | *Fm-3m* | *Fm-3m* | *Fm-3m* |
| a (Å) | | 7.867(5) | 7.836(1) | 7.862(2) |
| V (Å$^3$) | | 487.0(1) | 481.2(1) | 485.9(4) |
| Secondary Phase | | $Ca_2Fe_2O_5$ | $SrMoO_4$ | CaO |
| Space Group | | *Pcmn* | *$I4_1/a$* | *Fm-3m* |
| Second Phase (%) | | 32 | 7.5 | 17 |
| a (Å) | | 5.568(4) | 5.359(1) | 4.810(1) |
| b (Å) | | 14.947(1) | 5.359(1) | 4.810(1) |
| c (Å) | | 5.458(4) | 11.93(1) | 4.810(1) |
| Sr/Ca | x | 0.5 | 0.5 | 0.25 |
| | y | 0.5 | 0.5 | 0.25 |
| | z | 0.5 | 0.5 | 0.25 |
| | $U_{iso}$ | 0.001(2) | 0.016(2) | 0.019(1) |
| Fe | x | 0 | 0 | 0 |
| | y | 0 | 0 | 0 |
| | z | 0 | 0 | 0 |
| | $U_{iso}$ | 0.053(5) | 0.013(6) | 0.008(2) |
| Fe/Mo | x | 0.5 | 0.5 | 0.5 |
| | y | 0.5 | 0.5 | 0.5 |
| | z | 0.5 | 0.5 | 0.5 |
| | $U_{iso}$ | 0.065(3) | 0.065(5) | 0.010(4) |
| O | x | 0.237(2) | 0.248(3) | 0.250(2) |
| | y | 0 | 0 | 0 |
| | z | 0.5 | 0.5 | 0 |
| | $U_{iso}$ | 0.081(4) | 0.081(4) | 0.018(2) |

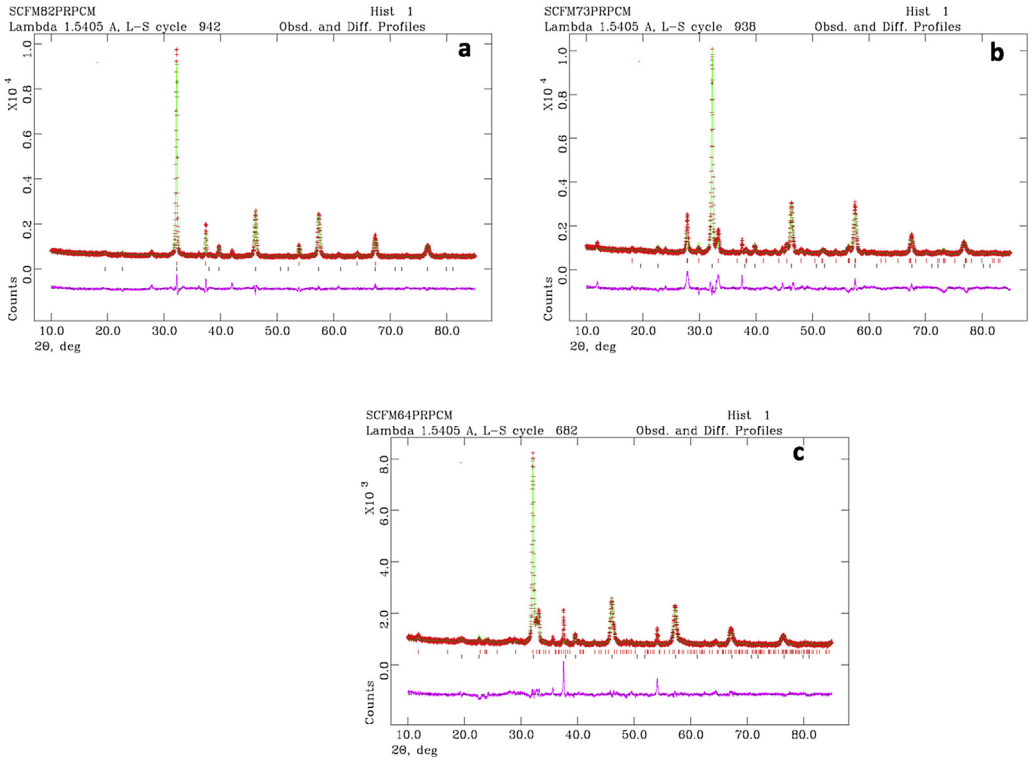


**Fig. 9.** GSAS plots of $SrCaFe_{1+x}Mo_{1-x}O_{6-\delta}$, x = 0.2 (a), x = 0.4 (b) and x = 0.6 (c) after re-oxidation and re-reduction of the samples reduced in 5% $H_2$/Ar at 1200 °C.

temperature reduction is expected to limit their utility as SOFC anode materials, as the vulnerability to oxidation can have disastrous consequence for fuel cell durability. As the redox stability of these materials was observed to increase with increasing iron content, further investigation into strontium ferrite materials was deemed to be a suitable avenue for further investigations.

## Acknowledgements

The authors thank EPSRC Flame SOFCs (EP/K021036/1), UK–India Biogas SOFCs (EP/I037016/1) and SuperGen Fuel Cells (EP/G030995/1) projects for funding. One of the authors (Cowin) thanks ScotChem SPIRIT scheme for support of his PhD study.

## References

[1] Y.-H. Huang, R.I. Dass, Z.-L. Xing, J.B. Goodenough, Science 312 (2006) 254–257.
[2] Q. Liu, X.H. Dong, G.L. Xiao, F. Zhao, F.L. Chen, Adv. Mater. 22 (2010) 5478–5482.
[3] S.W. Tao, J. Canales-Vazquez, J.T.S. Irvine, Chem. Mater. 16 (2004) 2309–2316.
[4] S.W. Tao, J.T.S. Irvine, J. Mater. Chem. 12 (2002) 2356–2360.
[5] S.W. Tao, J.T.S. Irvine, Nat. Mater. 2 (2003) 320–323.
[6] P. Zhang, Y.-H. Huang, J.-G. Cheng, Z.-Q. Mao, J.B. Goodenough, J. Power Sources 196 (2011) 1738–1743.
[7] L. Zhang, Q. Zhou, Q. He, T. He, J. Power Sources 195 (2010) 6356–6366.
[8] S. Vasala, M. Lehtimaki, Y.H. Huang, H. Yamauchi, J.B. Goodenough, M. Karppinen, J. Solid State Chem. 183 (2010) 1007–1012.
[9] A. Atkinson, S. Barnett, R.J. Gorte, J.T.S. Irvine, A.M. McEvoy, M. Mogensen, S.C. Singhal, J. Vohs, Nat. Mater. 3 (2004) 17–27.
[10] P.I. Cowin, C.T.G. Petit, R. Lan, J.T.S. Irvine, S.W. Tao, Adv. Energy Mater. 1 (2011) 314–332.
[11] G. Xiao, Q. Liu, X. Dong, K. Huang, F. Chen, J. Power Sources 195 (2010) 8071–8074.
[12] P.I. Cowin, R. Lan, C.T.G. Petit, S.W. Tao, Solid State Sci. 46 (2015) 62–70.
[13] A.C. Larson, R.B.V. Dreele, General Structural Analysis System, Los Alamos National Laboratory Report LAUR, 1994, p. 86.
[14] S.W. Tao, J.T.S. Irvine, J. Electrochem. Soc. 151 (2004) A252–A259.
[15] C.T. Petit, R. Lan, P.I. Cowin, J.T. Irvine, S.W. Tao, J. Mater. Chem. 21 (2011) 8854–8861.
[16] C.T.G. Petit, R. Lan, P.I. Cowin, J.T.S. Irvine, S.W. Tao, J. Mater. Chem. 21 (2011) 525–531.
[17] P.I. Cowin, R. Lan, L. Zhang, C.T.G. Petit, A. Kraft, S.W. Tao, Mater. Chem. Phys. 126 (2011) 614–618.
[18] J.A. Alonso, M.T. Casais, M.J. MartAnez-Lope, J.L. MartAnez, P. Velasco, A. Muoz, M.T. FernAndez-Daaz, Chem. Mater. 12 (1999) 161–168.
[19] G.Y. Liu, G.H. Rao, X.M. Feng, H.F. Yang, Z.W. Ouyang, W.F. Liu, J.K. Liang, J. Alloys Compd. 353 (2003) 42–47.
[20] Q. Liu, G.L. Xiao, T. Howell, T.L. Reitz, F.L. Chen, ECS Trans. 35 (2011) 1357–1366.
[21] D. Niebieskikwiat, R.D. Sanchez, A. Caneiro, L. Morales, M. Vasquez-Mansilla, F. Rivadulla, L.E. Hueso, Phys. Rev. B 62 (2000) 3340–3345.
[22] R.S. Liu, T.S. Chan, S. Mylswamy, G.Y. Guo, J.M. Chen, J.P. Attfield, Curr. Appl. Phys. 8 (2008) 110–113.
[23] C. Zener, Phys. Rev. 82 (1951) 403–405.
[24] A. Rosencwaig, Phys. Rev. 181 (1969) 946–948.
[25] Y. Yasukawa, J. Lindan, T.S. Chan, R.S. Liu, H. Yamauchi, M. Karppinen, J. Solid State Chem. 177 (2004) 2655–2662.
[26] P.W. Anderson, Phys. Rev. 109 (1958) 1492–1505.
[27] R. Allub, B. Alascio, Phys. Rev. B 55 (1997) 14113–14116.